

Performance of the Imaging Motional Stark Effect diagnostic at ASDEX Upgrade

A. Burckhart, O. Ford, A. Bock, R. Fischer, M. Reich, D. Rittich
and the ASDEX Upgrade team

Max-Planck Institut für Plasmaphysik, Garching / Greifswald, Germany

Introduction

Motional Stark Effect (MSE) diagnostics provide important information on the safety factor in magnetically confined fusion plasmas. They utilize the polarisation of Stark-split D-alpha light emitted by injected neutral particles. After being led through a set of two photo-elastic modulators, which modulate the intensity in time, this light is collected by the traditional MSE system via fibres defining individual lines of sight. Imaging MSE systems (IMSE), on the other hand, analyse the polarisation of those spectral components on a full image by guiding the light through a series of birefringent plates, combined with a linear polariser, before imaging it on a camera [fig. 1 left]. This leads to a spatial modulation which takes the form of an interference pattern in the image, containing both spatial and polarisation information in one single frame [fig. 1 centre]. After isolating three components from the 2D Fourier transform, the back-transformation yields an image of the polarisation angle of the MSE light [fig. 1 right].

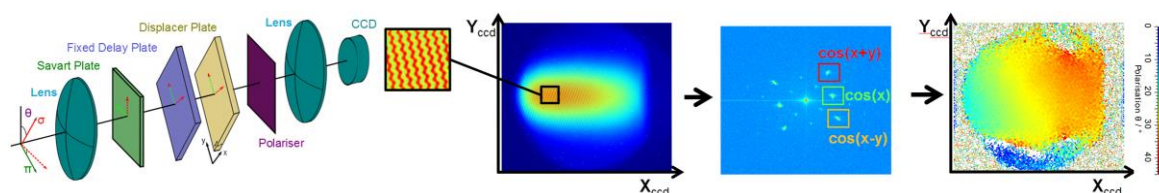


Figure 1: From left to right: A series of birefringent plates modulate incident polarised light to form an interference pattern on a camera chip. In the 2D FFT of this pattern three components are isolated and back-transformed to an image of the polarisation angle (right)

While conventional MSE systems filter out the π - or σ -lines of the Stark spectrum, the IMSE approach utilizes all of the lines, increasing the signal to noise ratio and eliminating the need for finely tuned narrow-band filters. Furthermore, IMSE is not disturbed by polarized broadband background light and provides a 2D image of the polarisation angle, increasing the quality of the equilibrium reconstruction compared to traditional 1D MSE systems.

The ASDEX Upgrade IMSE system and its performance

The ASDEX Upgrade (AUG) IMSE has a wide field of view, imaging from the outer separatrix to 10 cm across the magnetic axis. The optics are designed for low Faraday rotation. The stability of the analysis is monitored using in-vessel light sources with known polarisation. In the 2016 campaign a prototype “back-end” [1], which is the set of lenses and crystals creating the interference pattern, was mounted to the new optical in-vessel system.

While the system was installed to determine the requirements for a permanent solution, it already yielded a resolution of 0.1° in polarization angle at a time resolution of 5.6 ms, enabling the study of current redistribution during sawteeth [Fig 2 left]. In a comparison discharge with similarly sized sawteeth, the traditional MSE system was not able to resolve the crashes in the polarisation angle [Fig. 2 right].

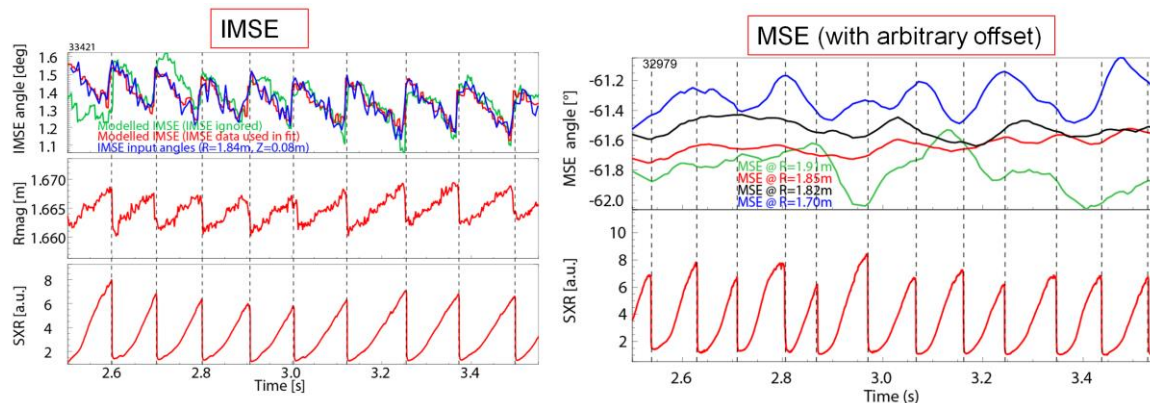


Figure 2: Response of the IMSE (left) and MSE (right) polarisation angles to sawtooth crashes

The left panels in figure 3 show a discharge in which the electron density increases from $6 \times 10^{19} \text{ m}^{-3}$ at 2.5s to $9 \times 10^{19} \text{ m}^{-3}$ at 4s. While the noise in the IMSE angle does increase with density, the agreement with the modelled values from the IDE equilibrium solver is still excellent [2].

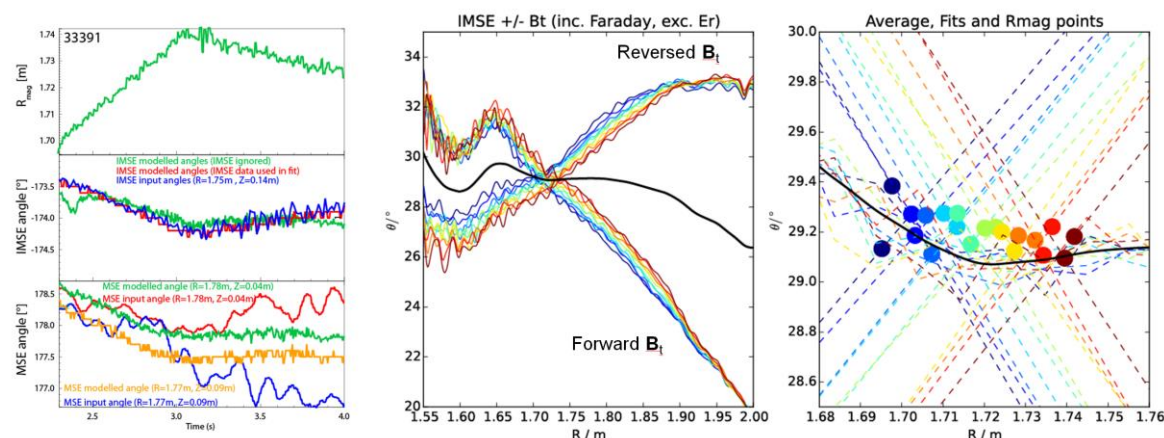


Figure 3: Left: comparison of the performance of IMSE and MSE at high densities. Centre: calibration of the angle offset using forward and reversed Bt discharges and comparison of the crossing point with the magnetic axis from CLISTE

Compared with the traditional MSE (Fig 3, left bottom plot), which runs into its limits due to polarised reflections at these high densities [3], the IMSE diagnostic performs very well under difficult conditions. However, the traditional MSE is currently being upgraded to an Alcator-C-mod-like polychromator based system [4] in order to solve the issues due to polarised reflections.

Calibration method and impact of IMSE data on equilibrium reconstruction

As the IMSE diagnostic is mounted to the entrance port of AUG and cannot be in position during the vessel opening, a calibration of the absolute angle offset from within the vessel is

not feasible. Therefore, we rely on an in-situ calibration using forward and reversed \mathbf{B}_t discharges to determine the angle offset. In identical discharges performed in both \mathbf{B}_t directions, the MSE angle decreases with radius in forward \mathbf{B}_t shots, while it increases in reversed \mathbf{B}_t [Fig. 3 centre]. The point at which the two curves cross each other corresponds to a zero poloidal contribution to the magnetic field, which defines the magnetic axis [5]. It can be seen in the right panel of figure 3 that this radial position agrees very well with the magnetic axis determined by the equilibrium solver CLISTE [6] (coloured dots). The different colours correspond to different time points in the R-scan shown in the top left panel.

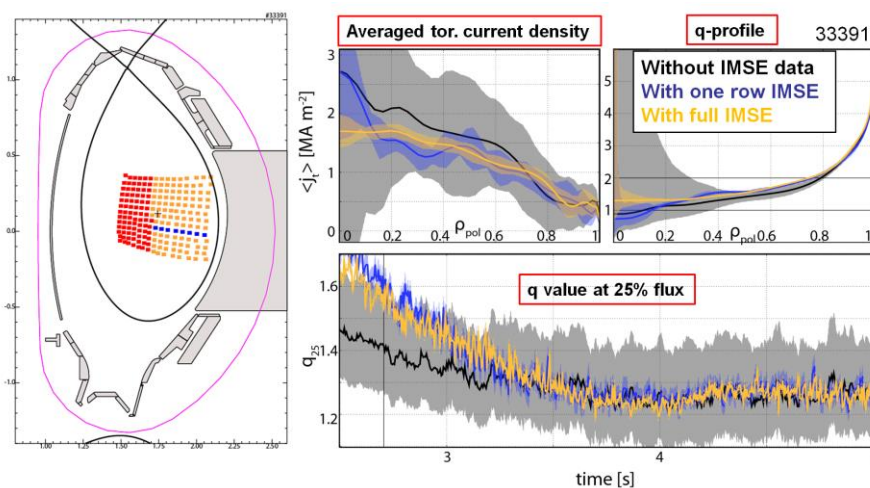


Figure 4: Spatial coverage of the IMSE (left) and reduction of the uncertainties by including its data in equilibrium solvers (right)

With the angle offset determined, the IMSE data can be used as a constraint in equilibrium solvers. Figure 4 shows the uncertainties in the toroidal current density and the safety factor q determined by IDE without IMSE constraints (black), with only 8 channels in one row (blue), and with a full 2D set of IMSE channels (orange). The quality of the equilibrium reconstruction improves immensely with the use of IMSE data. Note that the red channels in the left panel of figure 4 were ignored, as they were corrupted due to reflections occurring inside the IMSE system in the 2016 campaign. In the 2017 AUG campaign, all lenses and windows were anti-reflection coated, which improved the data quality in this region, but some corrupted data remained. As this corruption is believed to originate from an under dimensioned mirror in the vessel, the design has been adapted for the upcoming campaign.

The new IMSE backend

At the start of the 2017 campaign the prototype back-end was replaced by a fully optimized system [Fig 6 left]. The new design features larger birefringent plates yielding a larger étendue. The increase in light throughput is shown in figure 5 as the solid angle of the light reaching the camera from different radial locations in the beam. While the prototype system (range between cyan and black) only coupled roughly half of the light reaching the vacuum window (green), the new backend (red) manages to recouple nearly all the light. Compared to

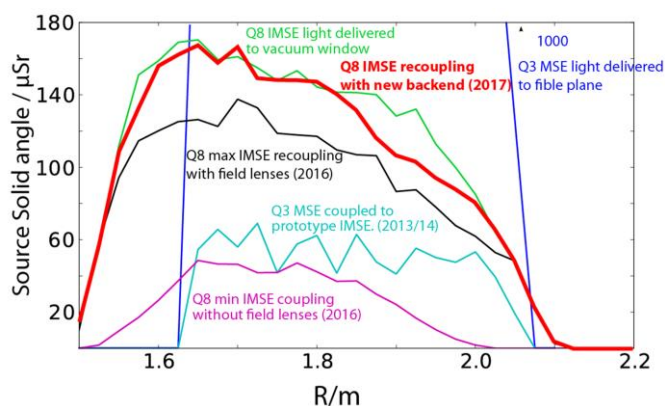


Figure 5: Light throughput of the prototype and new system

the optics of the traditional MSE system (blue, outside the plotted region), the light throughput is lower by a factor seven, since it was not possible to use a periscope based design similar to the MSE optics. The new system is built using a custom collimating lens to minimise Faraday rotation and has improved optimisation capabilities for field of view, vignetting and spectral range. The signal to noise level was significantly increased by the upgrade as is shown in the right panel of figure 6. While the sawteeth in the 2017 discharge were less pronounced and induced smaller changes in the polarisation angle, they are still clearly visible with less noise than in 2016.

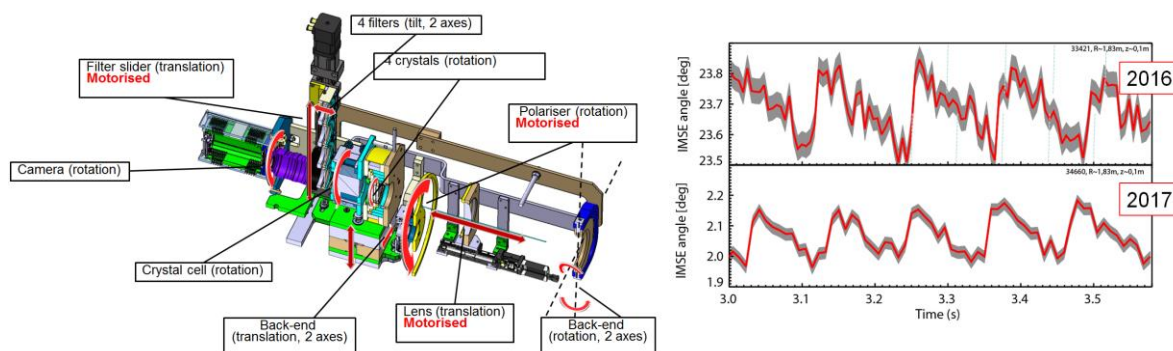


Figure 6: Left: new IMSE backend. Right: improvement in S/N ratio with the new backend

While the prototype system installed in 2016 already performed very well with its sensitivity exceeding expectations, the upgrade increased the performance even further. The absolute calibration of the IMSE system remains difficult as it relies on special discharges and a direct comparison with equilibrium solvers. Issues with the in-vessel polarised light sources prevented a validation of the Faraday model in 2017, but were solved for the upcoming campaign. The next steps include the validation of this model, and the routine evaluation of IMSE data to provide it as a standard input for equilibrium codes.

Acknowledgments: This work has been carried out within the framework of the EUROfusion Consortium and has received funding from the Euratom research and training programme 2014-2018 under grant agreement No 633053. The views and opinions expressed herein do not necessarily reflect those of the European Commission

References

- | | |
|--|---|
| [1] O. Ford, RSI 86, 093504 (2015) | [4] R. Mumgaard, RSI 87, 11E527 (2016) |
| [2] R. Fischer, FST 69, 526-536 (2016) | [5] O. Ford, RSI 87, 11E537 (2016) |
| [3] A. Bock, NF 57, 12 126041 (2017) | [6] P. McCarthy, PPCF 54, 1 015010 (2012) |